Supplement to:
The CAMS reanalysis of atmospheric composition

Antje Inness[1], Melanie Ades[1], Anna Agusti-Panareda[1], Jérôme Barré[1], Anna Benedictow[2], Anne-Marlene Blechschmidt[3], Juan Jose Dominguez[1], Richard Engelen[1], Henk Eskes[4], Johannes Flemming[1], Vincent Huijnen[4], Luke Jones[1], Zak Kipling[1], Sebastien Massart[1], Mark Parrington[1], Vincent-Henri Peuch[1], Miha Razinger[1], Samuel Remy[5], Michael Schulz[2] and Martin Suttie[1]

[1]ECMWF, Shinfield Park, Reading, RG2 9AX, UK
[2]Norwegian Meteorological Institute Postboks 43 Blindern, 0313 Oslo, Norway
[3]Institute of Environmental Physics, University of Bremen, Germany
[4]Royal Netherlands Meteorological Institute, De Bilt, The Netherlands
[5]IPSL, CNRS/UPMC, Paris, France

Correspondence to: Antje Inness (a.inness@ecmwf.int)

Monitoring of atmospheric composition data in the CAMS reanalysis

A closer look at the assimilated observations and their impact is obtained from timeseries of monthly mean analysis departures (i.e. observations minus analysis fields) and first-guess departures (i.e. observations minus model first guess) of the various retrievals. The first-guess is the model forecast initialised from the previous analysis. This allows us to assess how the analysis is drawing to the observations, and it also highlights problem periods of the observational data sets, for example changes in the data or periods without data. Here, we show such monitoring timeseries for all the assimilated atmospheric composition datasets, concentrating mainly on timeseries of monthly mean global mean departures, i.e. biases, and of standard deviation of departures.

The timeseries of departures for the TCO3 retrievals (SCIAMACHY, OMI, GOME-2A & GOME-2B) are shown in the main paper Figure 5. The remaining plots are shown here in the supplement, i.e. for the O_3 profile data in Figure S1 (MIPAS & MLS) and for the O_3 partial columns in Figure S2 (SBUV/2 NOAA-14 & NOAA-16) and Figure S3 (SBUV/2 NOAA-17, NOAA-18 & NOAA-19). For all four TCO3 data sets the analysis is drawing to the observations and the standard deviations of the analysis departures are reduced compared to those of the first-guess departures. The plots also show that the bias corrections (black lines) successfully adapt to changes in the data and remove the biases between total column data and the model, leading to small and stable bias corrected departures (dotted lines). Features that stand out for the O_3 retrievals are:

- Larger bias correction for SCIAMACHY in 2003 and early 2004 (Figure 5a). This points to a problem with the SCIAMACHY O_3 retrievals during the early Envisat operation.
- OMI data between 2009-2011 show a different behaviour than during the rest of the timeseries with larger departures (due to larger observation values, not shown) and the need for larger bias correction (Figure 5b). However, the VarBC successfully corrects for this and the bias corrected departures are small and stable. The reason for this change is a deterioration in the OMI row anomalies (Torres et al. 2018, see their Figure 1; Schenkeveld et al. 2017). Since June 2007 anomalous readings consisting of either an increase or decrease of radiance signal have affected individual OMI viewing positions (or rows) starting with rows 54 and 55, then spreading to rows 38-43 and from January 2009 extending to rows 28 - 45. Since then the behaviour of the row anomaly has remained dynamic. Which rows are affected and to what extent varies with time. Unfortunately, the row numbers are not given in the OMI Binary

Universal Form for the Representation of meteorological data (BUFR) files that were used as input for CAMSRA, so it was not possible to identify and blacklist individual rows.

- Increasing bias correction for GOME-2A with time, especially after January 2013 (Figure 5c) when the retrieval version changed from CCI v0100 to v0300 (see Table 2). GOME-2A spatial resolution changed from 40 km x 40 km to 40 km x 5 km after 15 July 2013. This could be a factor contributing to the increased need for bias correction from mid 2013 onwards, but cannot explain the increase at the beginning of 2013. The GOME-2A bias correction changes with season, with the largest correction (in the global mean) applied during boreal winter.
- Larger bias correction needed for GOME-2B than GOME-2A (Figure 5c and d)
- Much larger departures for the NRT MIPAS data (for the layer 10-20 hPa) used during 2003/4 than for the reprocessed MIPAS data from ESA's Climate Change Initiative (CCI) used after 2005 (Figure S1a), illustrating that the CCI data set is of much better quality than the original NRT data used for 2003/4. The MIPAS instrument was switched off in March 2004 due to a problem with moving retroreflectors and started to provide measurements again but at a reduced spectral resolution (about 40%) on a regular basis (but not continuously) from January 2005. Therefore, the CCI data are only available from 2005 onwards.
- Seasonally varying global mean departures of MLS with respect to the model (Figure S1b). MLS first-guess departures are negative for the 10-15 hPa layer in both polar regions and midlatitude regions (not shown). The largest negative first-guess and analysis departures are found during the summer months (i.e. boreal summer in NH, austral summer in SH) and the smallest ones during the respective winter seasons. This illustrates that the analysis can draw closer to the MLS data when no (or fewer) UV/VIS retrievals are assimilated. In the Tropics the departures are generally positive during the first months of the year and negative in the second half (not shown).
- Generally negative departures for NOAA-14, -16, -17 and -18 (Figures S2 and S3) in the layer 10-16 hPa.
- Change in departures for NOAA-14 during 2006 (Figure S3a). McPeters et al. (2013) states that the most stable instruments were those on NOAA 16, 17, and 18 and that the calibrations of the instruments on NOAA 14 are the most uncertain because of orbit drift and instrument problems.
- Smaller biases of NOAA-19 SBUV/2 compared to the other SBUV/2 retrievals until mid 2013 (Figure S3)
- The change in the biases of NOAA-16 and -19 in July 2013 arose because of changing from the offline 13 layer SBUV V8.6 product to a 21 layer NRT product (Figures S2 and S3).

Figure S4 shows timeseries of monthly mean departures for MOPITT TCCO averaged over the Globe and the NH midlatitudes. Like for O_3 the standard deviations of the departures are reduced as the analysis is drawing to the data. The global mean (Fig. S4a) is dominated by the Tropics and the SH where the departures are negative (observations smaller than model) and analysis departures are a lot smaller than the first-guess departures. In the NH (Fig. S4b) the departures are small (positive) during summer and larger (negative) during the winter. The CAMS model is known to have a negative bias in the lower troposphere at NH mid latitudes during winter (Flemming et al., 2017; Inness et al., 2015; CAMS NRT validation reports available from https://atmosphere.copernicus.eu/quality-assurance). At this time of year the sensitivity of MOPITT retrievals to CO in the lower troposphere is smaller than during summer because of reduced thermal contrast between the surface and the lower atmosphere (Deeter et al., 2013) and the MOPITT data cannot correct the CAMS model bias in the lower troposphere. An interesting result is that the standard deviation of both 'OBS-FG' and 'OBS-AN' reduces for more recent years, particularly over the NH midlatitudes from 2013 onwards, suggesting a better model representation of tropospheric CO for these later years compared to earlier years in this region.

The next two figures show the monthly mean departures for the tropospheric NO_2 columns from SCIAMACHY & OMI (Figure S5) and from GOME-2A & GOME-2B (Figure S6) averaged over the NH midlatitudes between 20ºN and 60ºN. This area was

chosen instead of the global mean because NO_2 values are highest and anthropogenic NO_2 emissions largest in the NH. Points to note for the NO_2 retrievals are:

- SCIAMACHY NO_2 departures are much larger in 2003 than during the other years (Figure S5a). As for O_3, this points to a problem with the retrievals in the early period after the Envisat launch. From 2004 onwards departures are largest during winter/spring and smallest during summer/autumn.
- OMI has a larger positive bias with respect to CAMS than the other NO_2 retrievals (Figure S5b). The bias correction removes most of this bias during the summer but to a lesser extent during the winter.
- Differences between GOME-2 analysis and first-guess departures are largest during the winter months when the NO_2 lifetime is longer and are shortest during the summer (Figure S6). During the summer months the standard deviations of the analysis departures hardly change compared to the first-guess departures illustrating that the data do not have much impact in the analysis. This was already noted by Inness et al. (2015) and illustrates the difficulty in using data assimilation to adjust the initial conditions of short lived species, such as NO_2.

Timeseries of monthly mean global mean departures for the AOD retrievals from MODIS Terra and Aqua are shown in Figure S7 and from AATSR in Figure S8. All three AOD retrievals have a positive bias with respect to CAMS. The bias correction removes the biases successfully leaving only small bias corrected first-guess departures. The main predictor for the aerosol VarBC is the wind speed over the ocean (Section 3.2). The analysis is drawing to the AOD retrievals and the standard deviation of the analysis departures is reduced compared to that of the first-guess departures.

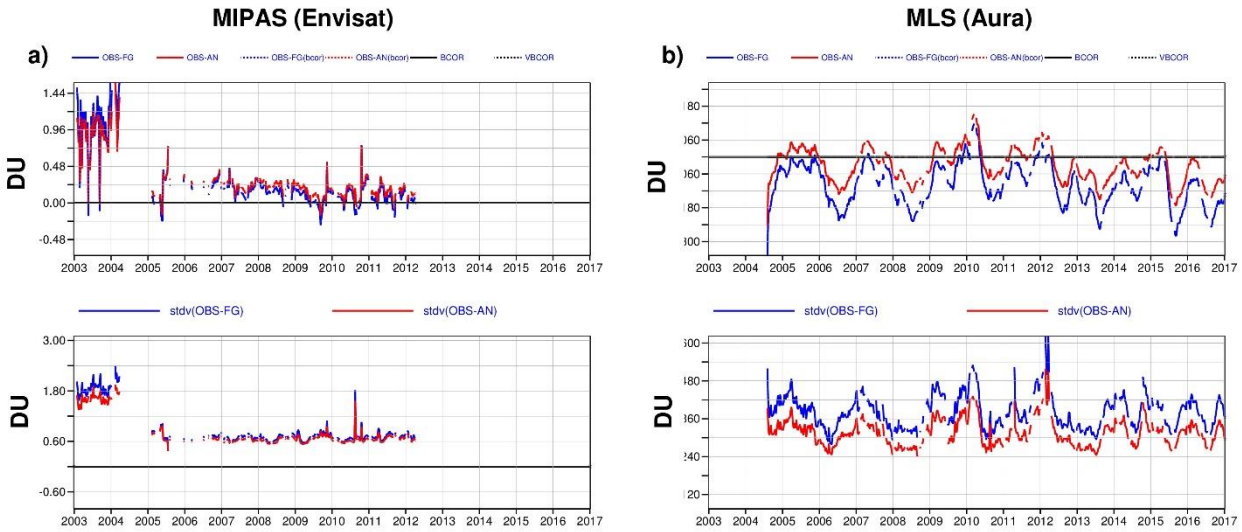

Figure S1: Timeseries of global mean monthly mean O_3 departures (top plots) and standard deviations of departures (bottom plots) of (a) MIPAS (layer between 10 and 20 hPa) and (b) MLS (layer between 10 and 14 hPa). The red lines show analysis departures, the blue lines first-guess departures, black lines bias correction and dotted red and blue lines the bias corrected analysis and first-guess departures, respectively. Values are in DU.

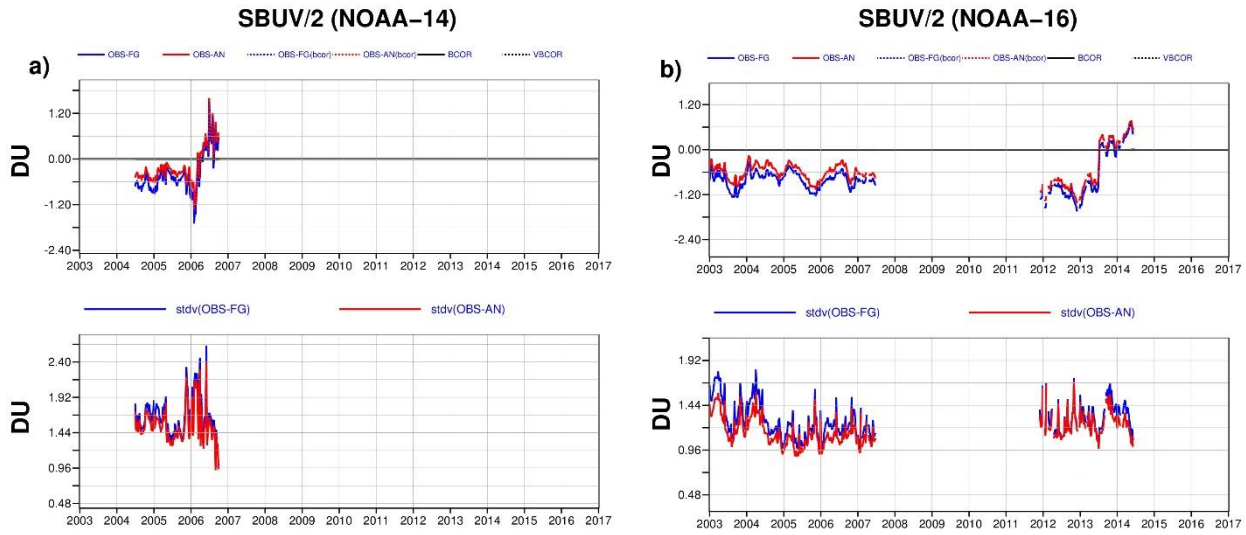

Figure S2: Like Figure S1 but for column O3 from SBUV-2 (layer between 10 and 16 hPa) from (a) NOAA-14 and (b) NOAA-16.

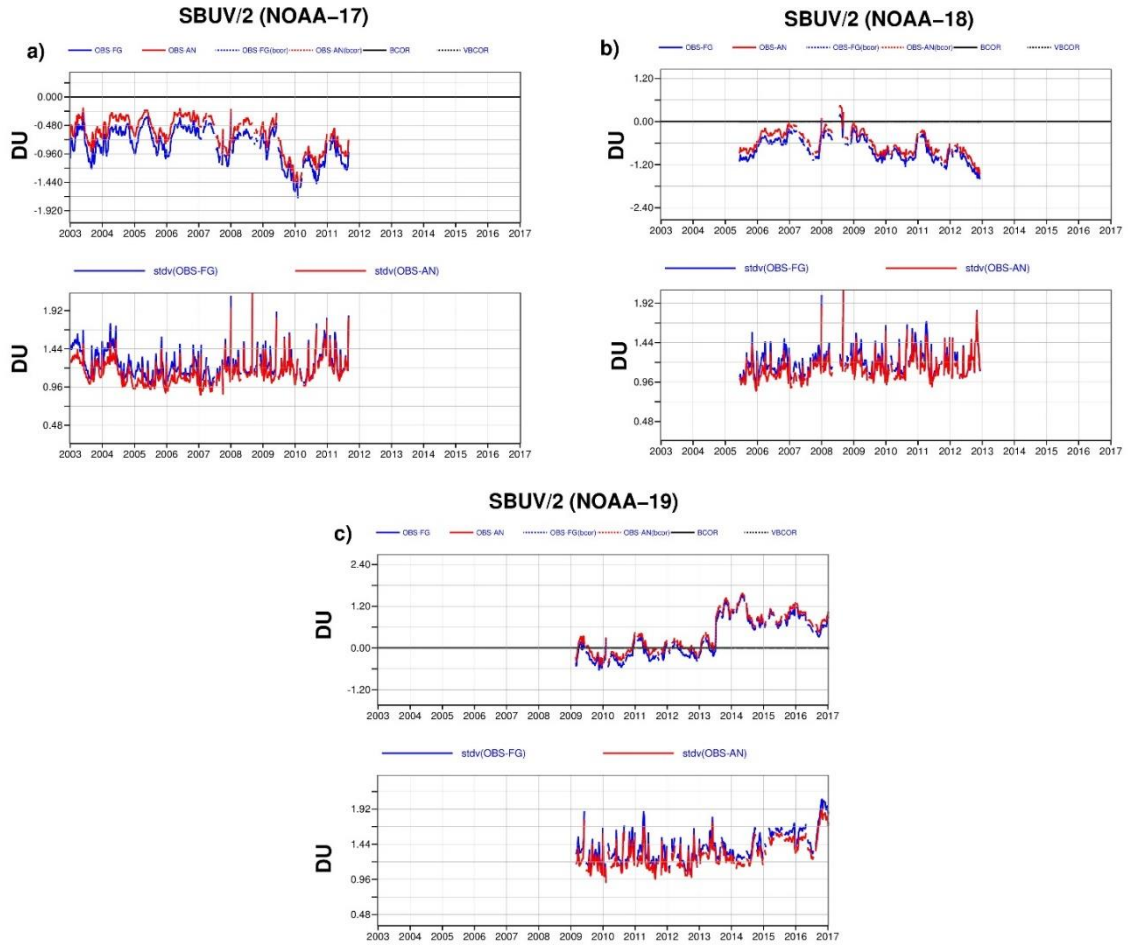

Figure S3: Like Figure S1 but for column O3 from SBUV-2 (layer between 10 and 16 hPa) from (a) NOAA-17, (b) NOAA-18 and (c) NOAA-19.

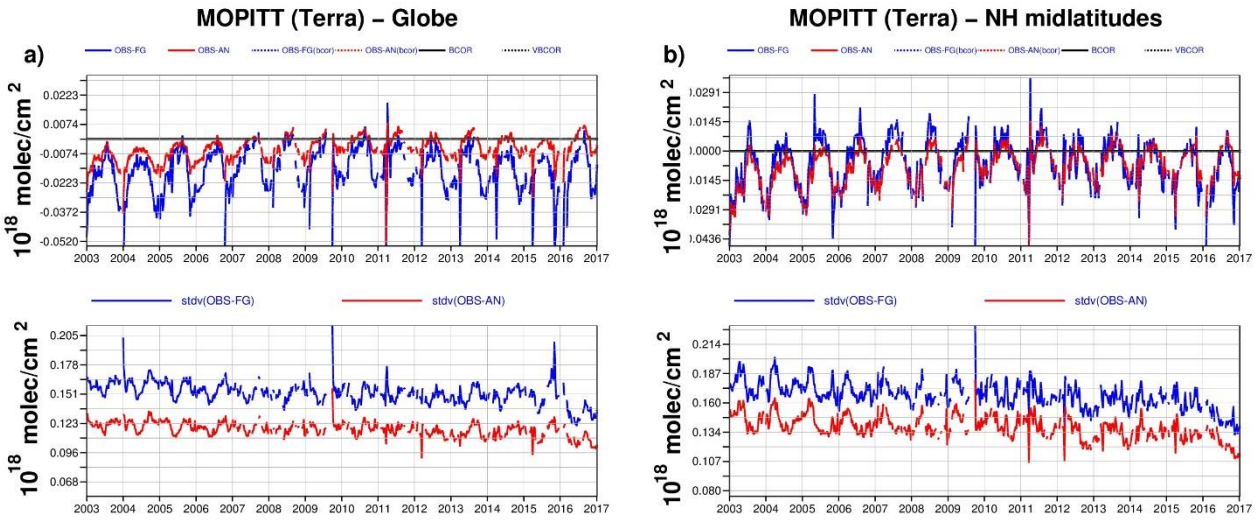

Figure S4: Like Figure S1 but for monthly mean TCCO departures from MOPITT in 10^{18} molec/cm^2: (a) shows global means, (b) means over the NH midlatitudes (20-60N).

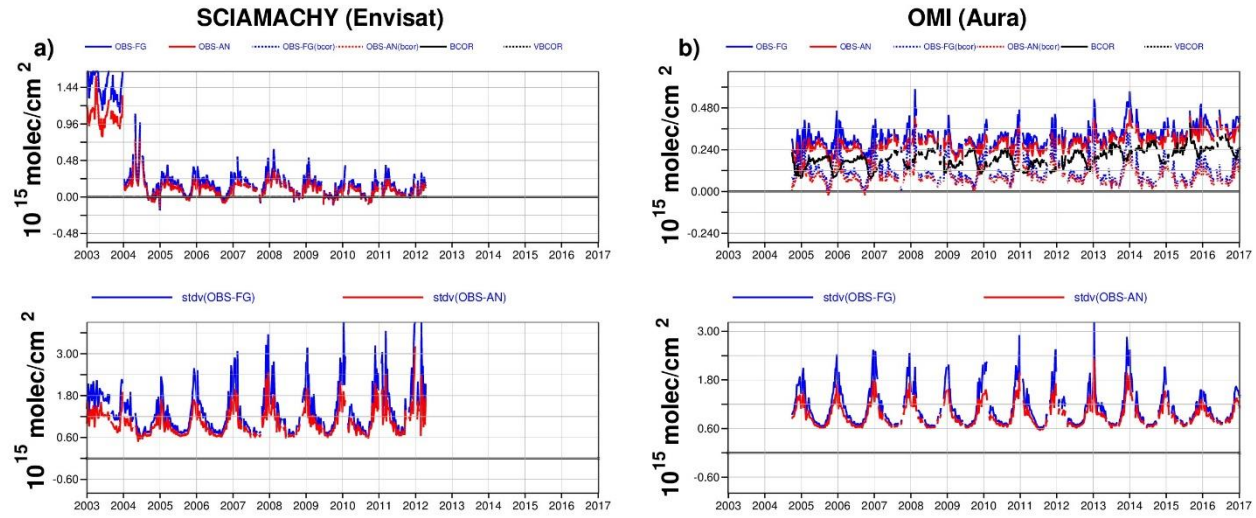

Figure S5: Like Figure S1 but for NO_2 from (a) SCIAMACHY and (b) OMI averaged over the NH (20-60ºN) in 10^{15} molec/cm^2.

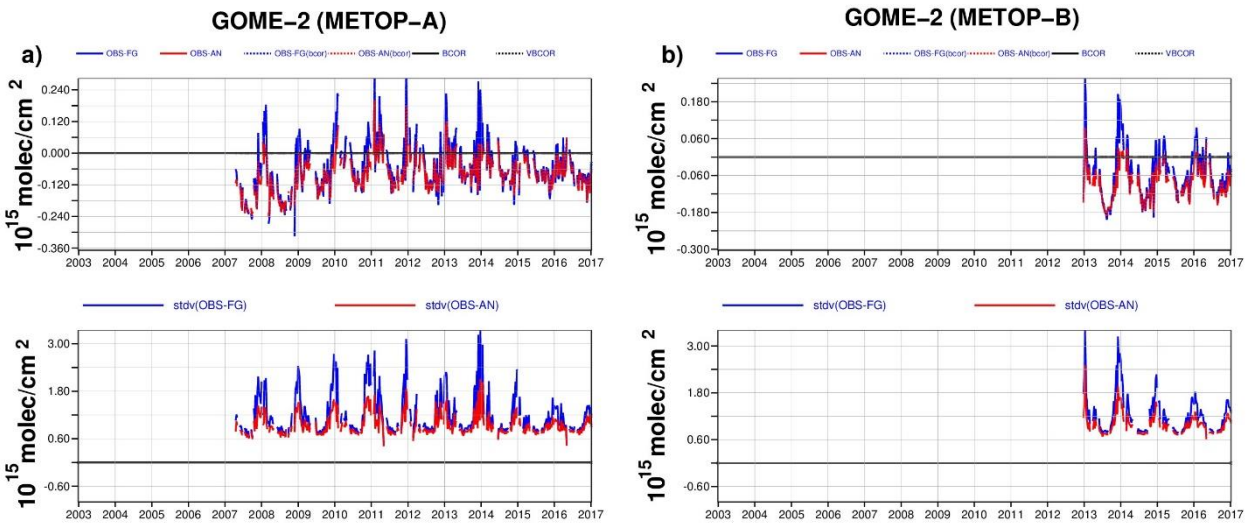

Figure S6: Like Figure S1 but for NO_2 from (a) GOME-2A and (b) GOME-2B averaged over the NH (20-60ºN) in 10^{15} molec/cm^2.

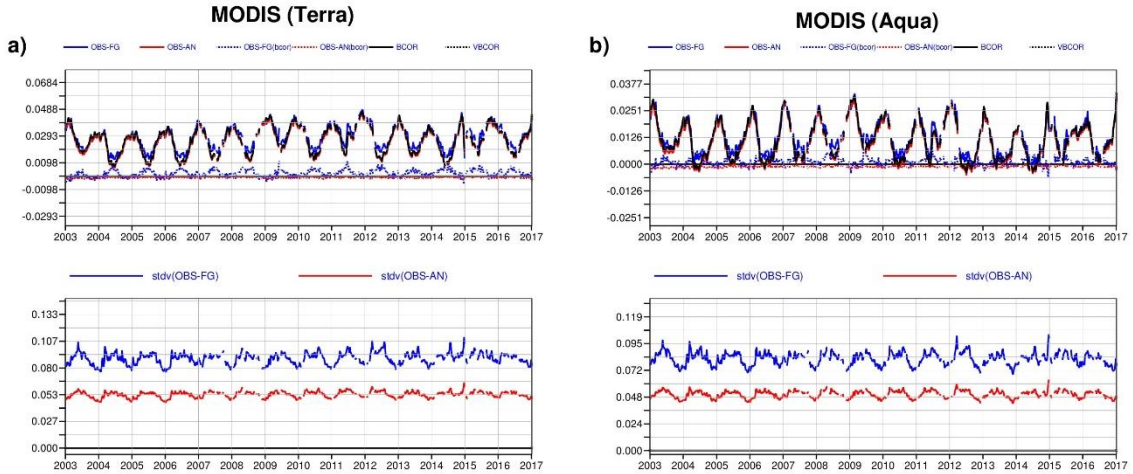

Figure S7: Like Figure S1 but for AOD from (a) Terra and (b) Aqua. AOD is unit less.

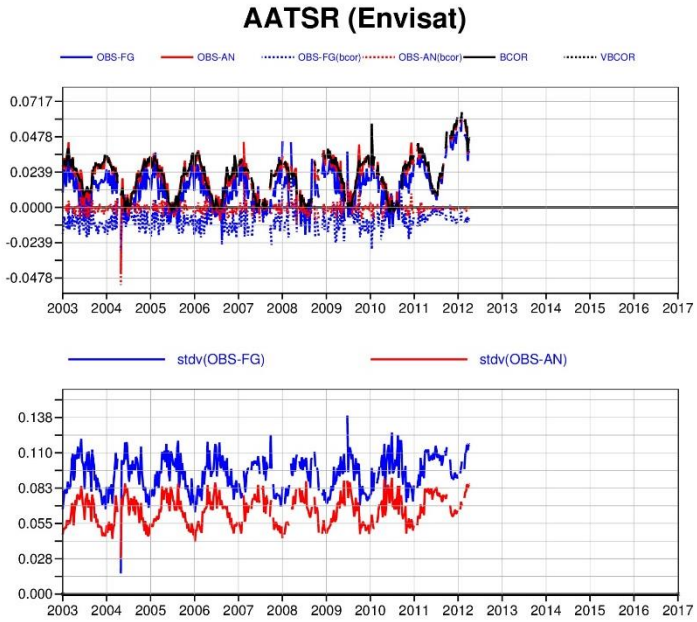

Figure S8: Like Figure S1 but for AOD from AATSR. AOD is unit less.

References

Deeter, M. N., S. Martínez-Alonso, D. P. Edwards, L. K. Emmons, J. C. Gille, H. M. Worden, J. V. Pittman, B. C. Daube, and S. C. Wofsy: Validation of MOPITT Version 5 thermal-infrared, near-infrared, and multispectral carbon monoxide profile retrievals for 2000–2011, J. Geophys. Res. Atmos., 118, 6710–6725, doi:10.1002/jgrd.50272, 2013.

Flemming, J., Benedetti, A., Inness, A., Engelen, R. J., Jones, L., Huijnen, V., Remy, S., Parrington, M., Suttie, M., Bozzo, A., Peuch, V.-H., Akritidis, D., and Katragkou, E.: The CAMS interim Reanalysis of Carbon Monoxide, Ozone and Aerosol for 2003–2015, Atmos. Chem. Phys., 17, 1945-1983, https://doi.org/10.5194/acp-17-1945-2017, 2017.

Inness, A., Blechschmidt, A.-M., Bouarar, I., Chabrillat, S., Crepulja, M., Engelen, R. J., Eskes, H., Flemming, J., Gaudel, A., Hendrick, F., Huijnen, V., Jones, L., Kapsomenakis, J., Katragkou, E., Keppens, A., Langerock, B., de Mazière, M., Melas, D., Parrington, M., Peuch, V. H., Razinger, M., Richter, A., Schultz, M. G., Suttie, M., Thouret, V., Vrekoussis, M., Wagner, A., and Zerefos, C.: Data assimilation of satellite-retrieved ozone, carbon monoxide and nitrogen dioxide with ECMWF's Composition-IFS, Atmos. Chem. Phys., 15, 5275-5303, doi:10.5194/acp-15-5275-2015, 2015.

Schenkeveld, V. M. E., Jaross, G., Marchenko, S., Haffner, D., Kleipool, Q. L., Rozemeijer, N. C., Veefkind, J. P., and Levelt, P.F.: In-flight performance of the Ozone Monitoring Instrument, Atmos. Meas. Tech., 10, 1957–1986, https://doi.org/10.5194/amt-10-1957-2017, 2017.

Torres, O., Bhartia, P. K., Jethva, H., and Ahn, C.: Impact of the ozone monitoring instrument row anomaly on the long-term record of aerosol products, Atmos. Meas. Tech., 11, 2701-2715, https://doi.org/10.5194/amt-11-2701-2018, 2018.